GEM - International Journal on Geomathematics (2019) 10:20
https://doi.org/10.1007/s13137-019-0132-8

ORIGINAL PAPER

Impact of heat generation/absorption on transient natural convective flow in an annulus filled with porous material subject to isothermal and adiabatic boundaries

Yusuf S. Taiwo[1] · **Gambo Dauda**[1]

Received: 7 February 2019 / Accepted: 23 August 2019 / Published online: 31 August 2019

Abstract
This article deliberated the effects of heat generation/absorption on transient natural convective flow in infinite vertical concentric cylinder filled with a porous material. The natural convective flow is as a result of constant heating at the inner cylinder while the inner surface of the outer cylinder is thermally insulated. A combination of Laplace transform technique and Riemann-sum approximation approach has been used to transform and invert the governing equation from the Laplace domain to the time domain respectively. The numerical values obtained from the Riemann-sum approximation excellently agree with the steady state solution at large time. The obtained results are represented graphically and the effects of the governing parameters on the velocity field, temperature field, mass flow rate, heat transfer as well as the skin-friction on both surfaces of the annulus are studied in detail. In the course of numerical computations, it is found that the fluid velocity and temperature both increases with time, while the fluid velocity and skin friction on both walls are seen to be proportional to Darcy number but inversely proportional to the viscosity ratio. Furthermore, it is found that the mass flow rate can be controlled by increasing/decreasing the heat generation/absorption parameter.

Keywords Transient · Isothermal · Adiabatic · Heat generation/absorption · Darcy number

Mathematics Subject Classification 76R10 · 76S05 · 76D05 · 75Q30 · 33C10 · 80A20 · 30E25

✉ Yusuf S. Taiwo
taiyeee@yahoo.com

Gambo Dauda
daudagambo85@gmail.com

[1] Department of Mathematics, Ahmadu Bello University, Zaria, Nigeria

List of symbols

t' Dimensional time (s)
r' Dimensional radial coordinate (m)
u' Axial velocity (m/s)
U Dimensionless axial velocity
R Dimensionless radial coordinate
T_0 Ambient temperature (K)
T_w Temperature of the hot cylinder (K)
θ Dimensionless temperature
r_1 Radius of the inner cylinder (m)
r_2 Radius of the outer cylinder (m)
g Gravitational acceleration (m/s^2)
V Dimensionless mass flow rate
Nu Dimensionless nusselt number
H Dimensionless heat generating/absorbing parameter
Q_0 Dimensional heat generating/absorbing parameter (K)
Pr Prandtl number ($\mu c_p/k$)
C_p Specific heat at constant pressure (kJ/kgK)
t Dimensionless time
K Permeability of the Porous medium (m^2)
k Thermal conductivity of the fluid (W/mK)
Da Darcy number

Greek letters

υ Fluid kinematic viscosity (m^2/s)
υ_{eff} Fluid kinematic effective viscosity (m^2/s)
τ Skin friction
ρ Density (Pa s)
η Laplace parameter
λ Ratio of radii (r_2/r_1)
γ Viscosity ratio
β Coefficient of thermal expansion

1 Introduction

Over the years, the study of transient free convective flow of viscous incompressible fluid in a vertical infinite concentric annulus has been investigated substantially by many researchers due to its industrial and technological applications such as in nuclear reactor cooling system, rapid cooling process, motion of fluid in computer equipment, radiators, storage devices, cooling of electronic equipment inside computers, furnaces, the growth of crystals for semiconductor industry most importantly when the convection current is induced by internal heat generation/absorption in addi-

tion to the heating at the outer surface of the inner cylinder. Many research work has been committed to study the effect of heat generation/absorption on convective flow in a channel, cylinder as well as annulus. In an attempt to generally examine the natural convective flow of a heat generating/absorbing fluid in an annulus (Jha and Yusuf 2017a) presented semi-analytical solution of transient natural convective flow of heat generation/absorption fluid in an annular porous medium. Later on, Yusuf and Jha (2018) investigated fully developed transient laminar natural convective flow of viscous, incompressible and heat generating/absorbing fluid in vertical concentric cylinders filled with porous material where the outer surface of the inner cylinder is heated constantly while the inner surface of the outer cylinder is maintained at constant temperature. In their work, it was observed that the effect of heat generation/absorption can be controlled by increasing/decreasing the viscosity ratio and there is an indication that heat generating fluid is desirable for optimum mass flux in the annular gap most importantly when the convection current is enhanced by constant heat flux. In another article, Yusuf (2017) analytically examined the laminar fully developed natural convective flow of an electrically conducting fluid in the vertical concentric annulus when the inner cylinder is heated or cooled either isothermally or at a constant heat flux while the inner surface of the outer cylinder is maintained at ambient temperature, (Al-Nimr and Darabseh 1995) presented the closed forms on transient fully developed free convection solutions, corresponding to four fundamental thermal boundary conditions in vertical concentric annulus. Recently, (Jha and Babatunde 2018) studied the natural convective flow with internal heat generation/absorption and found interesting results that skin friction and rate of heat transfer at the outer surface of the inner cylinder and inner surface of outer cylinder increases with increase in heat generation parameter while the reverse trend is found in the case of heat absorption parameter. In another related work, (Jha and Yusuf 2016) semi-analytically investigated the transient fully developed natural convection in an annular gap when the fluid is uniformly saturated with porous material. Similarly, (Jha and Odengle 2015) examined unsteady Couette flow in a composite channel partially filled with porous material. In order to establish the accuracy of the Riemann-sum approach used in their study, a numerical comparison with the implicit finite difference approach was presented with the aid of a table. In recent past, (Jha and Ajibade 2009) examined the influence of periodic heat input in fluid flowing in a vertical porous plate and later on considered the unsteady natural convective Couette flow of heat generating/absorbing fluid, (Jha and Ajibade 2010).

(Rachedi and Korti 2017) presented a numerical simulation of melting and solidification of different kinds of phase change material (PCM) encapsulated in spherical nodules in a water flow. The results indicate that natural convection dominates heat transfer during the charging mode while the solidification phase is conduction dominated in the discharging mode. Using numerical shooting technique with a fourth–fifth order Runge–Kutta scheme, (Eid 2016) carried out an investigation to study a problem of the chemical reaction and heat generation or absorption effects on MHD mixed convective boundary layer flow of a nanofluid through a porous medium due to an exponentially stretching sheet. It was found that Nusselt number is a decreasing function of the heat generation/absorption parameter and the chemical reaction parameter. Later, (Eid and Mahny 2017) examined the combined effects of magnetic field and heat generation/absorption on unsteady boundary-layer convective heat and mass transfer

of a non-Newtonian nanofluid over a permeable stretching wall and concluded that the thermal and concentration boundary-layer thickness has higher values with the increasing of magnetic field and heat generation in the case of a pseudoplastic nanofluid than others. (Eid et al. 2017) studied the characteristics of heat transfer of gold nanoparticles (Au-NPs) in flow past a power-law stretching surface. Sisko bio-nanofluid flow (with blood as a base fluid) in existence of non-linear thermal radiation. The study revealed that a better heat transfer is achieved as a result of the thermal radiation accretion which leads to deficiency in the thermal boundary-layer thickness. Finally, some remarkable problems studied by different researchers in this field can be seen in Eid and Mahny (2017), Inman (1962), Mahmoudi (2015), Jha and Yusuf (2017b), Jha et al. (2016), Moalem (1976) and Miyatake and Fujii (1972).

Hence, the purpose of this paper is to study the case when the fluid considered in the work of Jha and Yusuf (2017b) is filled with porous material. Retardation due to Lorentz force opposing fluid flow is negligible which is therefore neglected. In addition, for effective utilization of the available heat supplied to the system, the inner surface of the outer cylinder is insulated against heat this is to retain heat within the system.

2 Mathematical analysis

Consider a fully developed transient natural convective flow of an incompressible, viscous and heat generating/absorbing fluid within a vertical concentric annulus of infinite length. The convective current is as a result of the constant heating at the outer surface of the inner cylinder as well as the heat generating/absorbing nature of the fluid. The z'-axis is taken along the axis of the cylinder in the vertically upward direction opposite the gravitational force. The radius of inner and outer cylinders are denoted by r_1 and r_2 respectively as depicted in Fig. 1. Initially, at time $t' \leq 0$ the fluid and the two cylinders were assumed be at ambient temperature T_0. At $t' > 0$, the temperature at the outer surface of the inner cylinder changes to T_w while the outer surface of the outer cylinder is thermally insulated. The flow is thereby prompted by the buoyancy force arising from the temperature difference of the fluid in the annulus. Thus, under the usual Boussinesq approximation, the dimensionless form of the governing equations for the model under consideration can be written as

$$\frac{\partial U}{\partial t} = \gamma\left[\frac{\partial^2 U}{\partial R^2} + \frac{1}{R}\frac{\partial U}{\partial R}\right] - \frac{U}{Da} + \theta \tag{1}$$

$$\frac{\partial \theta}{\partial t} = \frac{1}{Pr}\left[\frac{\partial^2 \theta}{\partial R^2} + \frac{1}{R}\frac{\partial \theta}{\partial R}\right] + \frac{H\theta}{Pr} \tag{2}$$

The above equations have been rendered dimensionless using the following non-dimensional quantities:

$$t = \frac{t'\nu}{r_1^2}, \quad R = \frac{r'}{r_1}\lambda = \frac{r_2}{r_1} \quad \theta = \frac{(T' - T_0)}{T_w - T_0}, \quad Pr = \frac{\mu c_p}{k}$$

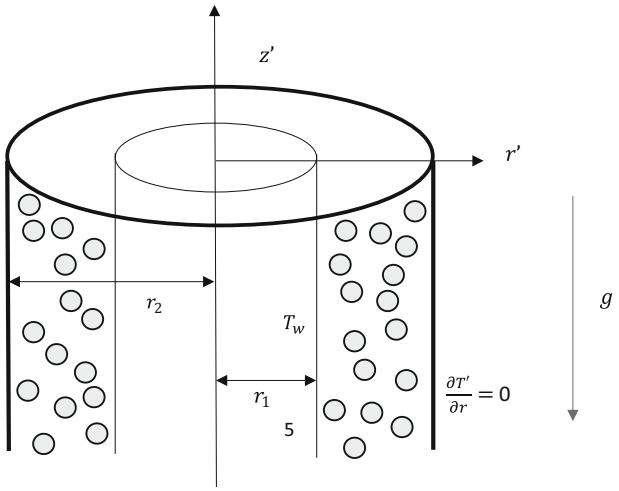

Fig. 1 Schematic diagram of the problem

$$\gamma = \frac{V_{eff}}{v}, \quad Da = \frac{K}{r_1^2}, \quad U = \frac{U'}{U_0}, \quad U_0 = \frac{g\beta(Tw - T_0)r_1^2}{v}, \quad H = \frac{Q_0 r_1^2}{k}$$

$$\gamma = \frac{V_{eff}}{v}, Da = \frac{K}{r_1^2}, U = \frac{U'}{U_0}, U_0 = \frac{g\beta(Tw - T_0)r_1^2}{v}, \quad H = \frac{Q_0 r_1^2}{k} \tag{3}$$

While the initial and boundary conditions in dimensionless form are given as:

$$t \leq 0, U = \theta = 0, 1 \leq R \leq \lambda \tag{4}$$

$$t > 0 : \begin{cases} U = 0, \ \theta = 1 \quad at \ R = 1 \\ U = 0, \ \frac{\partial \theta}{\partial R} = 0 \quad at \ R = \lambda \end{cases} \tag{5}$$

Using $\bar{U}(R, \eta) = \int_0^\infty U(R, t)e^{-\eta t}dt$ and $\bar{\theta}(R, \eta) = \int_0^\infty \theta(R, t)e^{-\eta t}dt$ where η is the Laplace parameter and $\eta > 0$.

The Laplace transforms of Eqs. (1) to (5) are given as

$$\frac{d^2\bar{U}}{dR^2} + \frac{1}{R}\frac{d\bar{U}}{dR} - \frac{1}{\gamma}\left[\frac{1}{Da} + \eta\right]\bar{U} + \frac{\bar{\theta}}{\gamma} = 0 \tag{6}$$

$$\frac{d^2\bar{\theta}}{dR^2} + \frac{1}{R}\frac{d\bar{\theta}}{dR} - [\eta \Pr - H]\bar{\theta} = 0 \tag{7}$$

Subject to

$$\bar{U} = 0; \ \bar{\theta} = \frac{1}{\eta} \quad \text{at } t = 1 \tag{8}$$

$$\bar{U} = 0; \ \frac{d\bar{\theta}}{dR} = 0 \quad \text{at } R = \lambda \tag{9}$$

The solutions of the Bessel ordinary differential equations in Eq. (6) and (7) in the Laplace domain subject to the boundary conditions (8) and (9) are given below

$$\bar{\theta}(R,\eta) = A_1 I_0(R\delta) + A_2 K_0(R\delta) \tag{10}$$

$$\bar{U}(R,\eta) = B_1 I_0(R\alpha) + B_2 K_0(R\alpha) - \frac{1}{\gamma}\left[\frac{A_1 I_0(R\delta) + A_2 K_0(R\delta)}{(\delta^2-\alpha^2)}\right] \tag{11}$$

where

$$\delta = \sqrt{\eta Pr - H}, \quad \alpha = \left[\frac{1}{\gamma}\left(\frac{1}{Da}+\eta\right)\right]^{1/2}, \quad A_1 = \frac{K_1(\lambda\delta)}{\eta[I_1(\lambda\delta)K_0(\delta) + I_0(\delta)K_1(\lambda\delta)]},$$
$$A_2 = \frac{I_1(\lambda\delta)}{\eta[I_1(\lambda\delta)K_0(\delta) + I_0(\delta)K_1(\lambda\delta)]}, \quad B_1 = \frac{M_2 K_0(\alpha) - M_1 K_0(\lambda\alpha)}{I_0(\lambda\alpha)K_0(\alpha) - I_0(\alpha)K_0(\lambda\alpha)},$$
$$B_2 = \frac{M_1 I_0(\lambda\alpha) - M_2 I_0(\alpha)}{I_0(\lambda\alpha)K_0(\alpha) - I_0(\alpha)K_0(\lambda\alpha)}.$$

2.1 Skin frictions, Nusselt number and mass flux

Using Eq. (11), the skin friction at the surface of the cylinders in the Laplace domain at $R = 1$ and $R = \lambda$ are given respectively as follows:

$$\tau_1(1,\eta) = \left.\frac{d\bar{U}}{dR}\right|_{R=1} = \alpha\{B_1 I_1(\alpha) - B_2 K_1(\alpha)\} - \frac{\delta}{\Upsilon}\frac{[A_1 I_1(\delta) - A_2 K_1(\delta)]}{(\delta^2-\alpha^2)} \tag{12}$$

$$\tau_\lambda(\lambda,\eta) = \left.\frac{d\bar{U}}{dR}\right|_{R=\lambda} = \alpha\{B_1 I_1(\lambda\alpha) - B_2 K_1(\lambda\alpha)\} - \frac{\delta}{\Upsilon}\frac{[A_1 I_1(\lambda\delta) - A_2 K_1(\lambda\delta)]}{(\delta^2-\alpha^2)} \tag{13}$$

Using Eq. (10) the rate of heat transfer at the surface of the inner cylinder in the Laplace domain is given by:

$$\bar{N}u_1 = \left.\frac{d\bar{\theta}}{dR}\right|_{R=1} = \delta[A_1 I_1(\delta) - A_2 K_1(\delta)] \tag{14}$$

Thus, the solution of the mass flow rate in the Laplace domain through the annular region is given by:

$$\bar{V} = 2\pi\int_1^\lambda R\bar{U}\,dR = 2\pi\left\{\left[\frac{B_1}{\alpha}(\lambda I_1(\lambda\alpha) - I_1(\alpha)) - \frac{B_2}{\alpha}(\lambda K_1(\lambda\alpha) - K_1(\alpha))\right]\right.$$
$$\left. - \frac{1}{\delta\Upsilon(\delta^2-\alpha^2)}[A_1(\lambda I_1(\lambda\delta) - I_1(\delta)) - A_2(\lambda K_1(\lambda\delta) - K_1(\delta))]\right\} \tag{15}$$

It is pertinent to note that the given solutions above are in Laplace domain. Equations (10)–(15) is to be transformed to the time domain. Due to the complex nature of

these solutions, the Riemann-sum approximation approach was adopted. Following the work of Jha and Yusuf (2016), any function in the Laplace domain can be inverted to the time domain as follows:

$$Z(R,t) = \frac{e^{\eta t}}{t}\left[\frac{1}{2}\bar{Z}(R,\eta) + \mathrm{Re}\left(\sum_{n=1}^{M}\bar{Z}\left(R, \varepsilon + \frac{in\pi}{t}\right)\right)(-1)^n\right] \tag{16}$$

where Z represents θ, U, Q or Nu as the case may be, Re refers to the real part of the summation, $i = \sqrt{-1}$, M is the number of terms used in the Riemann-sum approximation and ε is the real part of the Bromwich contour that is used in inverting Laplace transforms. The Riemann-sum approximation for the Laplace inversion involves a single summation for the numerical process its accuracy depends on the value of ε and the truncation error dictated by M. According to (Tzou 1997), the value of εt that best satisfied the result is 4.7.

2.2 Validation of the method

To validate the numerical technique employed in inverting Eqs. (10)–(15) to the time domain, the steady state solution of Eqs. (1) and (2) is computed, this is achieved by computing the steady state velocity field analytically which is expected to be in sync with transient state solution at large time. This is achieved by taking $\frac{\partial()}{\partial t} = 0$ in the non-dimensional Eqs. (1) and (2) which then reduces to the ordinary differential equations given by:

$$\gamma\left[\frac{d^2U}{dR^2} + \frac{1}{R}\frac{dU}{dR}\right] - \frac{U}{Da} + \theta = 0 \tag{17}$$

$$\frac{d^2\theta}{dR^2} + \frac{1}{R}\frac{d\theta}{dR} + H\theta = 0 \tag{18}$$

with the given boundary conditions

$$U = 0;\ \theta = 1 \quad \text{at } R = 1 \tag{19}$$

$$U = 0;\ \frac{d\theta}{dR} = 0 \quad \text{at } R = \lambda \tag{20}$$

Equations (17) and (18) are solved under the boundary conditions (19) and (20) to obtain the solution of the steady state temperature field, velocity field, skin friction on the surface of the cylinders, Nusselt number and mass flow rate. The solutions are given as;

$$\theta = C_1 J_0\left(R\sqrt{H}\right) + C_2 Y_0\left(R\sqrt{H}\right) \tag{21}$$

$$U = D_1 I_0\left(R\sqrt{\frac{1}{\gamma Da}}\right) + D_2 K_0\left(R\sqrt{\frac{1}{\gamma Da}}\right) + \frac{\left[C_1 J_0\left(R\sqrt{H}\right) + C_2 Y_0\left(R\sqrt{H}\right)\right] Da}{(H\gamma Da + 1)} \tag{22}$$

$$\tau_1 = \left.\frac{dU}{dR}\right|_{R=1} = \sqrt{\frac{1}{\gamma Da}}\left\{D_1 I_1\left(\sqrt{\frac{1}{\gamma Da}}\right) - D_2 K_1\left(\sqrt{\frac{1}{\gamma Da}}\right)\right\} + \sqrt{-H}\frac{\left[C_1 J_1\left(\sqrt{H}\right) - C_2 Y_1\left(\sqrt{H}\right)\right] Da}{(H\gamma Da + 1)} \tag{23}$$

$$\tau_\lambda = -\left.\frac{dU}{dR}\right|_{R=\lambda} = -\left[\sqrt{\frac{1}{\gamma Da}}\left\{D_1 I_1\left(\lambda\sqrt{\frac{1}{\gamma Da}}\right) - D_2 K_1\left(\lambda\sqrt{\frac{1}{\gamma Da}}\right)\right\} + \sqrt{-H}\frac{\left[C_1 J\left(\lambda\sqrt{H}\right) - C_2 Y_1\left(\lambda\sqrt{H}\right)\right] Da}{(H\gamma Da + 1)}\right] \tag{24}$$

$$Nu_1 = \left.\frac{d\theta}{dR}\right|_{R=1} = \sqrt{-H}\left\{C_1 I_1\left(\sqrt{-H}\right) - C_2 K_1\left(\sqrt{-H}\right)\right\} \tag{25}$$

$$\begin{aligned} V = 2\pi\int_1^\lambda RU dR = 2\pi\Bigg\{ & D_1\sqrt{\gamma Da}\left[\lambda I_1\left(\lambda\sqrt{\frac{1}{\gamma Da}}\right) - I_1\left(\sqrt{\frac{1}{\gamma Da}}\right)\right] \\ & - D_2\sqrt{\gamma Da}\left[\lambda K_1\left(\lambda\sqrt{\frac{1}{\gamma Da}}\right) - K_1\left(\sqrt{\frac{1}{\gamma Da}}\right)\right] \\ & + \frac{Da}{\sqrt{-H}(H\gamma Da + 1)} C_1\left[\lambda I_1\left(\lambda\sqrt{-H}\right) - I_1\left(\sqrt{-H}\right)\right] \\ & - C_2\left[\lambda K_1\left(\lambda\sqrt{-H}\right) - K_1\left(\sqrt{-H}\right)\right]\Bigg\} \end{aligned} \tag{26}$$

where

$$C_1 = \frac{K_1\left(\lambda\sqrt{-H}\right)}{I_0\left(\sqrt{-H}\right)K_1\left(\lambda\sqrt{-H}\right) + I_1\left(\lambda\sqrt{-H}\right)K_0\left(\sqrt{-H}\right)}$$

$$C_2 = \frac{I_1\left(\lambda\sqrt{-H}\right)}{I_0\left(\sqrt{-H}\right)K_1\left(\lambda\sqrt{-H}\right) + I_1\left(\lambda\sqrt{-H}\right)K_0\left(\sqrt{-H}\right)}$$

$$D_1 = \frac{C_1 Da}{H\gamma Da + 1}, \quad D_2 = \frac{C_2 Da}{H\gamma Da + 1}$$

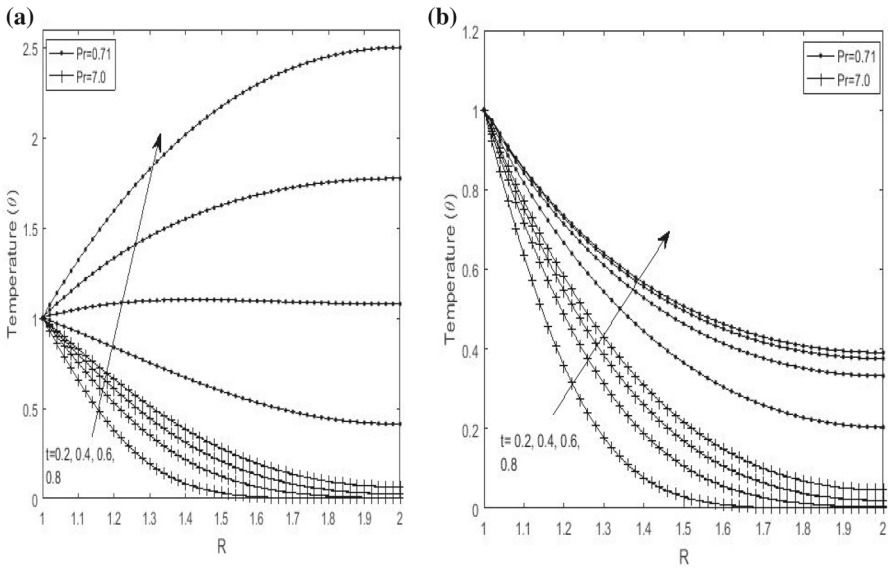

Fig. 2 Temperature variation for different values of $t(H = 2.0)$

3 Results and discussion

The solution of the present study obtained in the previous section are seen to be governed by heat generating/absorbing parameter (H), Darcy number (Da), Prandtl number (Pr), radius ratio (λ) and viscosity ratio (γ). The effect of these parameters on the fluid temperature, velocity, skin-friction are shown using the line graph while the numerical values for rate of heat transfer at the surface of the inner cylinder and mass flow rate were generated using the MATLAB program. The present parametric study has been carried out over a reasonable range $0.01 \leq Da \leq 1.0, 0.5 \leq \gamma \leq 1.5$, $-4 \leq H \leq 4$ where $\lambda = 2$ is also taken as reference point. All through this work, two values of Prandtl number ($Pr = 0.71$) and ($Pr = 7.0$) were considered which corresponds to air and water respectively. In the course of this research work, positive values of H shows that the fluid is generating heat and is specified as (a) in Figs. 2, 3, 4, 5, 6, 7, 8 and 9, while negatives values of H shows that the fluid is absorbing heat and is specified as (b) in Figs. 2, 3, 4, 5, 6, 7, 8 and 9.

Figure 2 shows the temperature variation with time (t). It is evident that temperature increases with increase in time, also there is higher temperature with slow convergence when $Pr = 7.0$ when the fluid is heat generating and the temperature decreases towards the outer cylinder in both (a) and (b) except when $Pr = 0.71$ in Fig. 2a. This further confirmed the findings reported in the previous works documented in the introductory session of this work that fluid temperature attains steady state faster when the fluid is heat absorbing. Generally, temperature is found to increase with decrease in Prandtl number.

Figure 3 depicts velocity variation for different values of time (t), it is noticed that the fluid velocity increases with time (t) when the fluid is either heat generating or

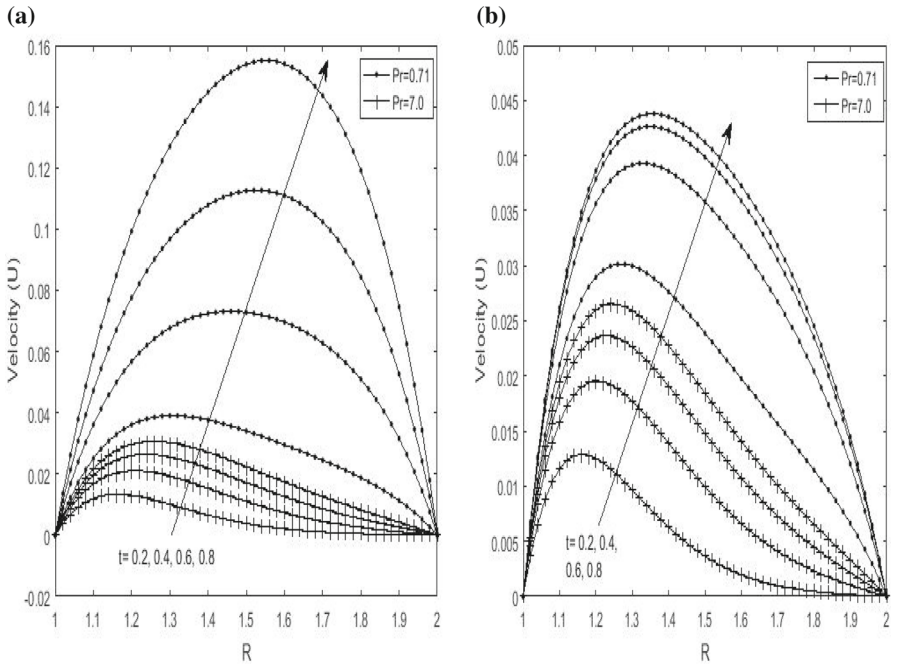

Fig. 3 Velocity variation for different values of $t(H = 2.0,\ Da = 0.1,\ \gamma = 0.5)$

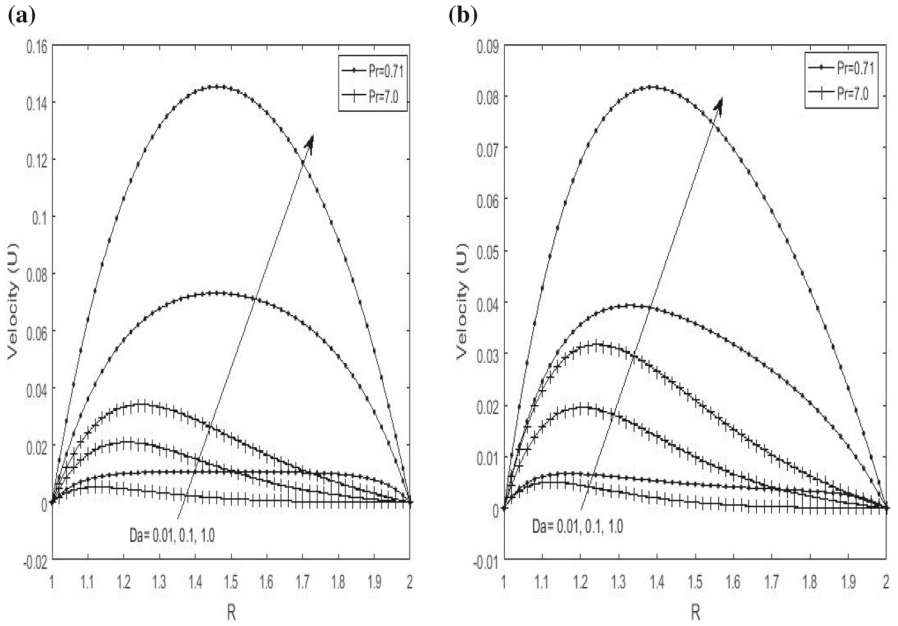

Fig. 4 Velocity variation for different values of $Da(H = 2.0, t = 0.4, \gamma = 0.5)$

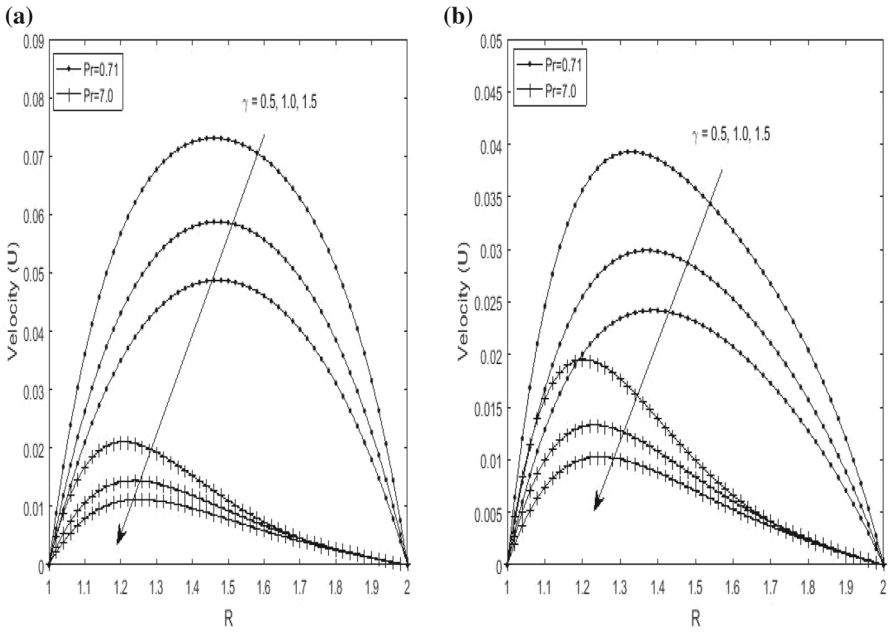

Fig. 5 Velocity variation for different values of $\gamma (H = 2.0, t = 0.4, Da = 0.1)$

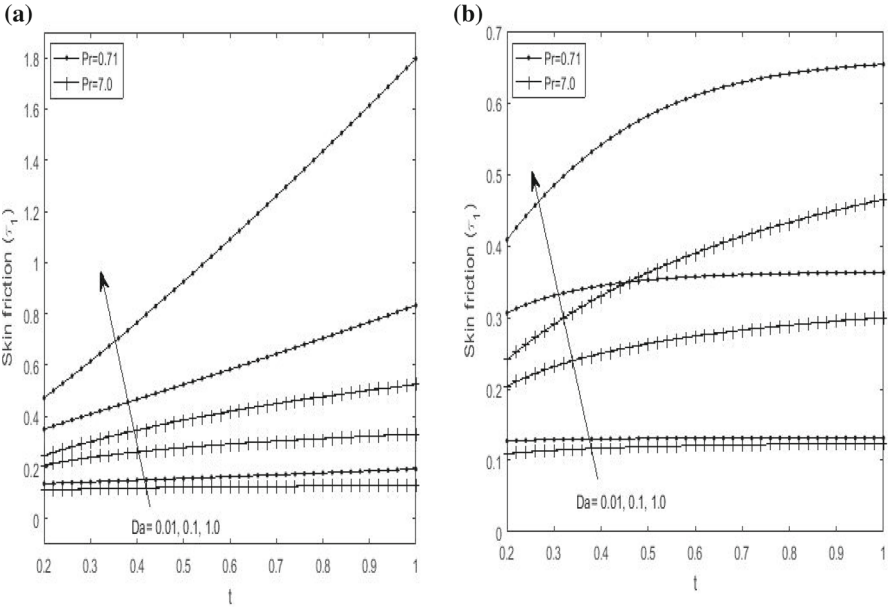

Fig. 6 Variation of skin friction (τ_1) for different values of $Da (H = 2.0, \gamma = 0.5)$

absorbing until the steady state is reached for both cases of (Pr). This is physically true since convection current is always higher in the case of air due to its low density in comparison to water. Moreover, the effect of the heat generation parameter on the

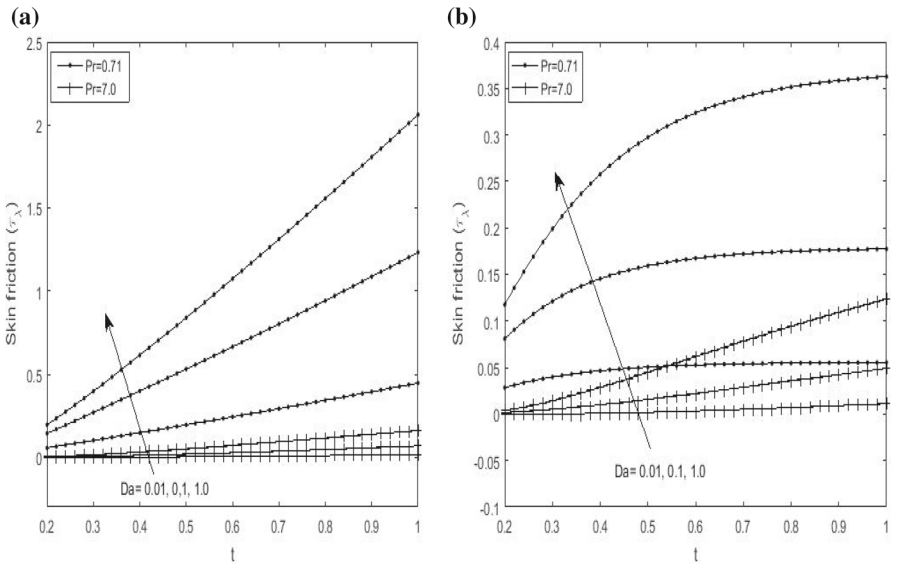

Fig. 7 Variation of skin friction (τ_λ) for different value of $Da(H = 2.0, \gamma = 0.5)$

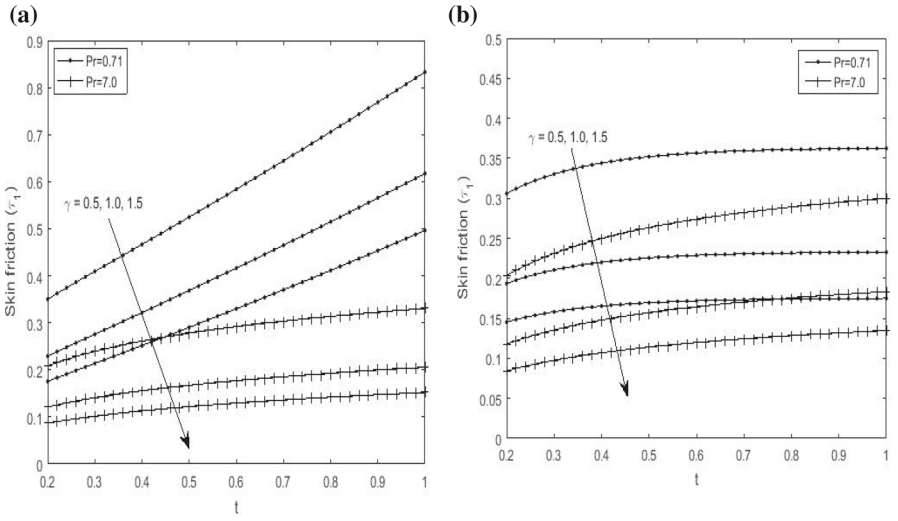

Fig. 8 Variation of skin friction (τ_1) for different value of $\gamma(H = 2.0, Da = 0.1)$

fluid velocity is more evident with increases in time, this can be linked to the fact that both heat generating parameter and the heating at the inner cylinder enhanced convective processes in the system.

The velocity variation for different values of Darcy number (Da) and the viscosity ratio (γ) is represented in Figs. 4 and 5 respectively. It is seen that there is a sharp increase in the fluid velocity when the fluid is heat generating as higher velocity

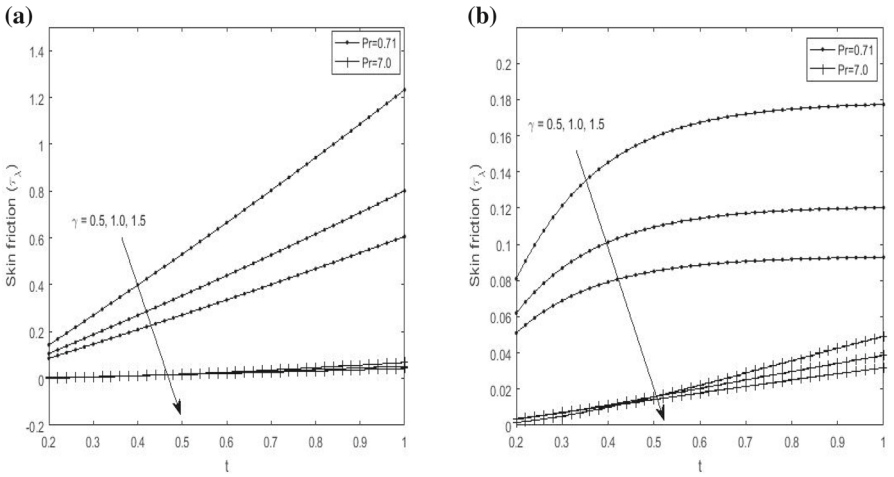

Fig. 9 Variation of skin friction (τ_λ) for different value of $\gamma (H = 2.0, Da = 0.1)$

profile are perceived in the annular gap when the fluid is heat generating. This can be attributed to the fact that as Darcy number (Da) increases, there is an equivalent increase in permeability of the porous materials. This further confirm the findings in the work of (Yusuf and Jha 2018). On the other hand, we see that with an upsurge in the viscosity ratio (γ), a corresponding decline in the fluid velocity in the annular gap with a much more decline when the fluid is heat absorbing is observed. Thus, we conclude that fluid velocity (U) is inversely proportional to the fluid viscosity ratio (γ).

Figures 6 and 7 reveal the combined effect of time (t), Darcy number (Da) and the viscosity ratio (γ) on the skin friction (τ_1) at the outer surface of the inner cylinder for both heat generating and absorbing flow. It is evident from Figs. 6 and 7 that the skin friction increases with time and Darcy number (Da). However the magnitude of skin friction (τ_1) is seen to be higher with heat generating fluid in comparison to the heat absorbing case (see Fig. 6b). In a similar fashion, skin friction (τ_λ) at the outer cylinder presented in Fig. 7a, b show a similar occurrence revealed in Fig. 6a, b respectively.

It can also be noticed that the magnitude of the skin friction is higher in the case of heat generation for the aforementioned cases. As it can be viewed clearly these figures show that skin friction is higher at the heated inner surface of the outer cylinder.

Figures 8 and 9 show the combined effect of the time (t), Prandtl number (Pr) and viscosity ratio (γ) on the skin frictions (τ_1) and (τ_λ) respectively for both heat generating and heat absorbing cases. Obviously, the figures revealed that skin friction decreases with increase in both Prandtl number and viscosity ratio. However, an increase in skin friction on both walls is obtained with time. It is interesting to note that skin friction on both walls attain steady state faster in the case of the heat absorption. It is good to also note that similar to the observation in Figs. 6 and 7, skin friction is observed to be higher at the heated inner cylinder.

The numerical values of the rate of heat transfer at the outer surface of the inner cylinder and fluid mass flow rate is presented in Tables 1 and 2 respectively. It is clear

Table 1 Numerical values for the Nusselt number ($R = 1, \lambda = 2$)

t	H	$Pr = 0.71$	$Pr = 7.0$
0.2	− 2.0	− 0.7126	0.1006
	− 1.0	− 0.4357	0.1948
	0.0	− 0.1314	0.2899
	1.0	0.2056	0.3860
	2.0	0.5815	0.4830
0.4	− 2.0	− 0.8334	− 0.1938
	− 1.0	− 0.4273	− 0.0622
	0.0	0.0733	0.0719
	1.0	0.7109	0.2086
	2.0	1.5503	0.3480
0.6	− 2.0	− 0.9153	− 0.3457
	− 1.0	− 0.4233	− 0.1864
	0.0	0.2497	− 0.0227
	1.0	1.2350	0.1458
	2.0	2.7807	0.3193

Table 2 Numerical values for mass flow rate ($\lambda = 2, Da = 0.1, \gamma = 1.0$)

t	H	$Pr = 0.71$	$Pr = 7.0$
0.1	− 2.0	21.2158	11.1251
	− 1.0	25.8206	11.6548
	0.0	30.9015	12.1878
	1.0	36.5222	12.7242
	2.0	42.7550	13.2640
0.2	− 2.0	28.6441	12.8547
	− 1.0	36.3520	13.6649
	0.0	45.6468	14.4856
	1.0	56.9580	15.3171
	2.0	70.8401	16.1595
0.3	− 2.0	32.7908	14.7625
	− 1.0	43.0922	15.8296
	0.0	56.5312	16.9182
	1.0	74.3976	18.0289
	2.0	98.5653	19.1624

in Table 1 that rate of heat transfer is inversely proportional to time for both heat generation and heat absorption. While mass flow rate is directly proportional to time for both cases. The mass flow rate is also seen to be higher in the case of air, this can be attributed to the low viscosity nature of air in comparison to water.

4 Conclusions

In this paper, a semi-analytical solution of the mathematical model accountable for the impact of heat generation/absorption on transient natural convective flow in an annulus filled with porous materials subject to isothermal and adiabatic boundaries has been considered in terms of both Bessel and modified Bessel functions of first and second kind. The effect of various flow parameter on the solution of the governing equations has been presented. The study revealed that the flow in the system can be controlled by selecting appropriate value of flow parameter as well as insulating the outer cylinder. This mechanism can be found in annular fin where heat loss is found to me maximum when fin is isothermal. It is also applicable in piping systems in engineering and boiler plant among others.

References

Al-Nimr, M.A., Darabseh, T.: Analytical solution for transient laminar fully developed free convection in open-ended vertical concentric porous annuli. J. Heat Transf. **17**(3), 762–765 (1995)

Eid, M.R.: Chemical reaction effect on MHD boundary-layer flow of two-phase nanofluid model over an exponentially stretching sheet with a heat generation. J. Mol. Liq. **220**, 718–725 (2016)

Eid, M.R., Alsaedi, A., Muhammad, T., Hayat, T.: Comprehensive analysis of heat transfer of gold-blood nanofluid (Sisko-model) with thermal radiation. Results Phys. **7**, 4388–4393 (2017)

Eid, M.R., Mahny, K.L.: Unsteady MHD heat and mass transfer of a non-Newtonian nanofluid flow of a two-phase model over a permeable stretching wall with heat generation/absorption. Adv. Powder Technol. **28**(11), 3063–3073 (2017)

Inman, R.M.: Experimental study of temperature distribution in laminar tube flow of a fluid with internal heat generation. Int. J. Heat Mass Transf. **5**, 1053 (1962)

Jha, B.K., Ajibade, A.O.: Free convection flow of heat generation/absorption fluid between vertical porous plates with periodic heat input. Int. Commun. Heat Mass Transf. **36**, 624–631 (2009)

Jha, B.K., Ajibade, A.O.: Unsteady free convective Couette flow of heat generating/absorbing fluid. Int. J. Energy Technol. **2**, 1–9 (2010)

Jha, B.K., Babatunde, A.: Investigation of heat generation/absorption on natural convection flow in a vertical annular micro-channel: an exact solution. Multidiscip. Model. Mater. Struct. 143–167 (2018)

Jha, B.K., Odengle, J.O.: Unsteady Couette flow in a composite channel partially filled with porous material: a semi-analytical approach. Transp. Porous Media **107**, 219–234 (2015)

Jha, B.K., Oni, M.O., Aina, B.: Steady fully developed mixed convection flow in a vertical micro-concentric annulus with heat generating/absorbing fluid: an exact solution. Ain Shams Eng. J. (2016)

Jha, B.K., Yusuf, T.S.: Transient free convective flow in an annular porous medium: a semi-analytical approach. Eng. Sci. Technol. Int. J. (2016)

Jha, B.K., Yusuf, T.S.: Transient free convective flow with heat generation/absorption in an annular porous medium: a semi-analytical approach. J. Process Mech. Eng. (2017a)

Jha, B.K., Yusuf, T.S.: MHD transient free convection flow in vertical concentric annulus with isothermal and adiabatic boundaries. Int. J. Eng. Technol. **52**, 40–52 (2017b)

Mahmoudi, Y.: Constant wall heat flux boundary condition in micro-channels filled with a porous medium with internal heat generation under local thermal non-equilibrium condition. Int. J. Heat Mass Transf. **85**, 524–542 (2015)

Miyatake, O., Fujii, T.: Free convection heat transfer between vertical plates - one plate isothermally heated and other thermally insulated. Heat Transf. Jpn. Res. **1**, 30–38 (1972)

Moalem, D.: Steady state heat transfer with porous medium with temperature dependent heat generation. Int. J. Heat Mass Transf. **19**, 529 (1976)

Rachedi, K., Korti, A.I.N.: Numerical simulation of melting and solidification of different kinds of phase change materials (PCM) encapsulated in spherical nodules in a water flow. Comput. Thermal Sci. **9**(4), 283–296 (2017)

Tzou, D.Y.: Macro to microscale heat transfer: the lagging behavior. Taylor and Francis, London (1997)

Yusuf, T.S.: Exact solution of an MHD natural convection flow in vertical concentric annulus with heat absorption. Int. J. Fluid Mech. Thermal Sci. **3**, 52–61 (2017)

Yusuf, T.S., Jha, B.K. A semi-analytical solution for time dependent natural convection flow with heat generation/absorption in an annulus partially filled with porous material. Multidiscip. Model. Mater. Struct. (2018)